

To appear in The Astrophysical Journal Letters

Observational evidence of spin-induced precession in active galactic nuclei

Anderson Caproni¹, Herman J. Mosquera Cuesta ²,

and

Zulema Abraham¹

ABSTRACT

We show that it is possible to explain the physical origin of jet precession in active galactic nuclei (AGNs) through the misalignment between the rotation axes of the accretion disk and of the Kerr black hole. We apply this scenario to quasars, Seyfert galaxies and also to the Galactic Center black hole Sgr A*, for which signatures of either jet or disk precession have been found. The formalism adopted is parameterized by the ratio of the precession period to the black hole mass and can be used to put constraints to the physical properties of the accretion disk as well as to the black hole spin in those systems.

Subject headings: accretion, accretion disks — black hole physics — galaxies: active — galaxies: jets — relativity

1. Introduction

It is a well-accepted idea that the center of an AGN harbors a supermassive black hole surrounded by an accretion disk, the dynamics of which eventually produces a bipolar jet. In some AGNs, there were found evidence of disk precession. In Seyfert galaxies this precession was detected, in direct form, from the variability of double-peaked Balmer lines (e.g., Storchi-Bergmann et al. 2003). In blazars, where the accretion disk emission is overrun by the non-thermal jet emission, precession can be inferred indirectly from the jet kinematics (ejection of superluminal knots in distinct directions and with different apparent proper motions) or from periodic boosting of the continuum emission (e.g., Abraham 2000; Caproni & Abraham 2004a).

¹Instituto de Astronomia, Geofísica e Ciências Atmosféricas, Universidade de São Paulo, R. do Matão 1226, Cidade Universitária, CEP 05508-900, São Paulo, SP, Brazil; acaproni@astro.iag.usp.br, zulema@astro.iag.usp.br.

²Instituto de Cosmologia, Relatividade e Astrofísica (ICRA-BR), Centro Brasileiro de Pesquisas Físicas, R. Dr. Xavier Sigaud 150, CEP 22290-180, Rio de Janeiro, RJ, Brazil; hermanjc@cbpf.br.

A question that could be arisen is: what is the physical mechanism driving the disk precession? In Seyfert galaxies, precession has been attributed to the relativistic advance of the pericenter in an elliptical accretion disk (e.g., Eracleous et al. 1995), to the precessing single-spiral arm in a circular disk (e.g., Storchi-Bergmann et al. 2003), or to a radiation-induced warp in the disk (e.g., Pringle 1996; Storchi-Bergmann et al. 1997). For blazars, several authors have proposed a binary black hole system scenario wherein the primary accretion disk precesses due to torques induced by the secondary black hole, whose orbital plane does not coincide with that of the accretion disk (Sillanpää et al. 1988; Lehto & Valtonen 1996; Katz 1997; Romero et al. 2000; Stirling et al. 2003; Caproni & Abraham 2004a,b). Although supermassive binary black hole systems provide precession periods compatible with observations, the mean separation of the black holes might be sometimes substantially short, so that their timescale for coalescence might reach less than 1000 years (Caproni 2004).

In this work, we discuss the possibility that the disk precession arises from torques induced by the misalignment between the angular momenta of a Kerr black hole and that of the accretion disk, which can be applied both to blazars and Seyfert galaxies. In § 2, we derive the relation between precession period, mass of the black hole and physical parameters of the accretion disk. In § 3 we apply this formalism to several objects for which precession period and black hole mass are known, and in § 4 we present our conclusions.

2. Spin-induced disk precession

Frame dragging produced by a Kerr black hole, known as Lense-Thirring effect (Lense & Thirring 1918), leads a particle to precess if its orbital plane is inclined in relation to the equatorial plane of the black hole (the angular momentum of the black hole is perpendicular to this plane). The amplitude of the precession angular velocity ω_{L-T} decreases with the cube of the distance (e.g., Wilkins 1972) and becomes negligible at large distances.

If a viscous accretion disk is inclined in relation to the equatorial plane of the Kerr black hole, the differential precession will produce warps in the disk. The combined action of the Lense-Thirring effect and the internal viscosity of the accretion disk forces the alignment between the angular momenta of the Kerr black hole and the accretion disk. This is known as the Bardeen-Petterson effect (Bardeen & Petterson 1975) and affects only the innermost part of the disk, while its outer parts tend to remain in its original configuration, due to the short range of the Lense-Thirring effect. The transition radius between these two regimes is known as Bardeen-Petterson radius, and its exact location depends on the Mach number of the accretion disk (Bardeen & Petterson 1975; Kumar & Pringle 1985; Scheuer & Feiler 1996; Ivanov & Illarianov 1997; Nelson & Papaloizou 2000).

Nelson & Papaloizou (2000) studied numerically the time evolution of an accretion disk due to the Bardeen-Petterson effect produced by a maximally rotating black hole, and found that the

initial differentially precessing disk evolves towards a rigid-body-like precession. Thus, we will assume hereafter that the accretion disk precesses as a rigid-body.

In the reference frame precessing with the accretion disk, the total torque \vec{T} due to the Bardeen-Petterson effect acting upon the misaligned accretion disk is given by (Papaloizou & Terquem 1995):

$$\vec{T} = \frac{d\vec{L}_d}{dt} + \omega_{\text{prec}} \frac{\vec{J}_{\text{BH}}}{|\vec{J}_{\text{BH}}|} \times \vec{L}_d, \quad (1)$$

where \vec{L}_d and ω_{prec} are respectively the total angular momentum of the disk and the precession angular velocity, \vec{J}_{BH} is the angular momentum of the black hole, defined as $|\vec{J}_{\text{BH}}| = GM_{\text{BH}}^2 |a_*|/c$, G is the gravitational constant, M_{BH} the mass of the black hole and c the light speed. The dimensionless parameter a_* ($-1 \leq a_* \leq 1$) is the ratio of the angular momentum of the compact object and that of a Kerr black hole rotating at its maximal velocity. The signs “+” and “-” correspond respectively to prograde and retrograde black hole rotation relative to the angular velocity of the accretion disk.

In the Kerr metric, the radius of the marginally stable orbit R_{ms} , which will be taken as the inner radius of the accretion disk, is given by $R_{\text{ms}} = \xi_{\text{ms}} R_g$, where $R_g = GM_{\text{BH}}/c^2$ is the gravitational radius, $\xi_{\text{ms}} = 3 + A_2 \mp \sqrt{(3 - A_1)(3 + A_1 + 2A_2)}$, with $A_1 = 1 + (1 - a_*^2)^{1/3} [(1 + a_*)^{1/3} + (1 - a_*)^{1/3}]$ and $A_2 = \sqrt{3a_*^2 + A_1^2}$. In this case, the minus and plus signs correspond to prograde and retrograde motion, respectively.

When the system reaches a quasi-stationary state, the precession period of the disk, P_{prec} , is given in the source’s reference frame by (Liu & Melia 2002):

$$P_{\text{prec}} = 2\pi \sin \theta \left(\frac{L_d}{T} \right), \quad (2)$$

where θ is the angle between the orientations of the angular momenta of the black hole and that of the accretion disk. Assuming that the surface density of the disk Σ_d depends only on the radius r and that there is no warping in the disk, L_d can be written as:

$$L_d = 2\pi \int_{R_{\text{ms}}}^{R_{\text{out}}} \Sigma_d(r) \Omega_K(r) r^3 dr, \quad (3)$$

where R_{out} is the outer radius of the precessing part of the disk and Ω_K is the relativistic Keplerian angular velocity, given as:

$$\Omega_{\text{K}}(r) = \frac{c^3}{GM_{\text{BH}}} \left[\left(\frac{r}{R_{\text{g}}} \right)^{3/2} + a_* \right]^{-1}. \quad (4)$$

For small precession angles θ , T can be represented by (Liu & Melia 2002):

$$T = 4\pi^2 \sin \theta \int_{R_{\text{ms}}}^{R_{\text{out}}} \Sigma_{\text{d}}(r) \Omega_{\text{K}}(r) \nu_{\text{p}\theta}(r) r^3 dr, \quad (5)$$

with the nodal precession frequency $\nu_{\text{p}\theta}$ given by (Kato 1990):

$$\nu_{\text{p}\theta} = \frac{\Omega_{\text{K}}(r)}{2\pi} \left[1 - \sqrt{1 - 4a_* \left(\frac{R_{\text{g}}}{r} \right)^{3/2} + 3a_*^2 \left(\frac{R_{\text{g}}}{r} \right)^2} \right]. \quad (6)$$

Substituting equations [4] and [6] into equations [3] and [5], and introducing the dimensionless variable $\xi = r/R_{\text{g}}$, we obtain:

$$P_{\text{prec}} = \left(\frac{2\pi GM_{\text{BH}}}{c^3} \right) \frac{\int_{\xi_{\text{ms}}}^{\xi_{\text{out}}} \Sigma_{\text{d}}(\xi) [\Upsilon(\xi)]^{-1} \xi^3 d\xi}{\int_{\xi_{\text{ms}}}^{\xi_{\text{out}}} \Sigma_{\text{d}}(\xi) \Psi(\xi) [\Upsilon(\xi)]^{-2} \xi^3 d\xi}, \quad (7)$$

with $\xi_{\text{out}} = R_{\text{out}}/R_{\text{g}}$, $\Upsilon(\xi) = \xi^{3/2} + a_*$ and $\Psi(\xi) = 1 - \sqrt{1 - 4a_*\xi^{-3/2} + 3a_*^2\xi^{-2}}$.

This equation is parametrized by the relation between the precession period and the black hole mass, which depends on the black hole spin and on how the disk surface density varies with radius. In this work, we shall adopt two different descriptions for this last parameter: a power-law function, such as $\Sigma_{\text{d}}(\xi) = \Sigma_0 \xi^s$ (e.g., Papaloizou & Terquem 1995; Larwood 1997; Nelson & Papaloizou 2000), and an exponential function $\Sigma_{\text{d}}(\xi) = \Sigma_0 e^{\sigma\xi}$ (e.g., Stehle & Spruit 2001; D’Angelo, Henning & Kley 2003), where Σ_0 , s and σ are arbitrary constants.

3. Predictions from the spin-induced precession model for an AGN sample

In Figure 1, we show the iso-contours of the ratio $P_{\text{prec}}/M_{\text{BH}}$ calculated from equation [7] in the $[\log(R_{\text{out}}/R_{\text{ms}}), a_*]$ -plane. The integrals in that equation were calculated for values of R_{out} between 1.1 and $1000R_{\text{ms}}$.¹

¹The extent of the outer edge of an accretion disk is controversial. For instance, Collin-Souffrin & Dumont (1990) assumed an accretion disk that extends up to about $10^5 R_{\text{g}}$, while Goodman (2003) argue that, due to self-gravity, the outer parts of the disk might fragmentise, reducing its size to about $2000R_{\text{g}}$.

The calculations were performed for values of a_* between -1 and 1.² We have considered both power-law and exponential profiles for the surface density using four different values of s (-2, -1, 0 and 2) and for σ (-2, -1, 0 and 0.05).³

One can see that the general behaviour of $P_{\text{prec}}/M_{\text{BH}}$ depends strongly on the accretion disk structure (s or σ), specially in the case of exponential disks. Indeed, if we maintain a_* fixed, the increase of $P_{\text{prec}}/M_{\text{BH}}$ with R_{out} occurs at a higher rate as s or σ increases. In some cases when $\sigma < 0$, $P_{\text{prec}}/M_{\text{BH}}$ tends asymptotically to a constant value that, on the other hand, will be reached at lower values of R_{out} and $|a_*|$ as σ becomes more negative. This is a consequence of the rapid decrease of the amount of disk material with the distance in such configurations. Indeed, this trend is also seen in power-law disks with $s < -2$.

For a particular $R_{\text{out}}/R_{\text{ms}}$, the same value of $P_{\text{prec}}/M_{\text{BH}}$ is obtained for a smaller absolute value of a_* in the case of prograde rotation, giving an asymmetry in the curves shown in Figure 1. This can be explained if we consider that in this case, the inner disk boundary is closer to the gravitational radius, where the Lense-Thirring effect is more prominent.

To compare the model predictions with observations we analysed a set of sources for which information of both precession periods and black hole masses are available. The selected sources correspond to the Seyfert I galaxies NGC 1097 and 3C 120, the broad-line radio galaxy Arp 102B, the BL Lac OJ 287, the quasars 3C 273, 3C 279 and 3C 345, and the Galactic Center source Sgr A*⁴, whose parameters and references are listed in Table 1.

The dashed lines in Fig. 1 correspond to the values of $P_{\text{prec}}/M_{\text{BH}}$ for each object listed in Table 1. One can note that there is always a set of parameters (a_* , s/σ , R_{out}) capable of reproducing the precession period related to the sources in both disk models, indicating that the spin-induced precession can be a feasible engine for disk/jet precession. However, not all the disk models and sizes can provide precession periods as those found in our sample of AGN. This can put constraints on the physical parameters of the disks present in the AGNs for which evidence of precession were found. For instance, $P_{\text{prec}}/M_{\text{BH}}$ of the quasar 3C 345 is reproduced by the spin-induced precession model in the case of a power-law disk with $s = -2$ only if the black hole has a spin $a_* \leq -0.35$ or $a_* \geq 0.2$.

²Although Thorne (1974) has shown that $a_* \leq 0.998$ for a thin Keplerian disk due to the photon capture by the black hole, the black hole can spin up either by black hole mergers (Agol & Krolik 2000), or through accretion from a thick disk (Abromowicz & Lasota 1980).

³Accretion disk models found in the literature, such as those developed by Shakura & Sunyaev (1973), usually provide a radial dependency of the surface density in this range.

⁴Although our Galaxy is not exactly an AGN, the supermassive black hole in its center is a good candidate for this study since there are already a large number of observational and theoretical investigations on this source (e.g., Melia et al. 2001, Liu & Melia 2002, Liu & Melia 2003). Hence the validity of the model may be tested by combining the results here with other aspects of the source.

4. Conclusions

In this work we analyzed the possibility of jet/disk precession in AGNs be driven by torques in an accretion disk produced by the misalignment between the angular momenta of the black hole and that of the accretion disk. We adopted a formalism based on Liu & Melia (2002), and obtained an equation for the ratio of the precession period to the black hole mass, parametrized by the Kerr metric and the disk structure, which is mostly determined by physical processes, such as viscosity and radiation. This expression can be used to extract the physical properties of the accretion disk, as well as of the black hole spin in astrophysical systems that present signatures of disk/jet precession.

Two different disk models were used in the calculations: power law and exponential surface density profiles. We applied these models to eight objects for which precession periods and black hole masses are published. We showed that it is always possible to obtain a set of parameters that provides a jet/disk precession period compatible with those derived from high-resolution radio maps and continuum variability (e.g., Liu & Melia 2002; Caproni & Abraham 2004b), or from the double-peak emission-line variability (e.g., Newman et al. 1997; Storchi-Bergmann et al. 2003). However, not all the possible combinations of a_* , s/σ and R_{out} render results compatible with the observation, putting constraints on the disks properties if the precession is due to the proposed mechanism.

This work was supported by the Brazilian Agencies CNPq, FAPESP and FAPERJ. We would like to thank the anonymous referee for the useful commentaries and suggestions.

REFERENCES

- Abraham, Z., Carrara, E. A. 1998, A&AS, 496, 172.
- Abraham, Z., Romero, G. E. 1999, A&A, 344, 61.
- Abraham, Z. 2000, A&A, 355, 915.
- Abromowicz, M. A., Lasota, J. P. 1980, Acta Astron., 30, 35.
- Agol, E., Krolik, J. H. 2000, ApJ, 528, 161.
- Bardeen, J. M., Petterson, J. A. 1975, ApJ, 195, L65.
- Caproni, A. 2004, Ph.D. Thesis, Universidade de São Paulo.
- Caproni, A., Abraham, Z. 2004a, ApJ, 602, 625.
- Caproni, A., Abraham, Z. 2004b, MNRAS, 349, 1218.

- Collin-Souffrin, S., Dumont, A. M. 1990, *A&A*, 229, 292.
- D’Angelo, G., Henning, T., Kley, W. 2003, *ApJ*, 599, 548.
- Eracleous, M., Livio, M., Halpern, J. P., Storchi-Bergmann 1995, *ApJ*, 438, 610.
- Gu, M., Cao, X., Jiang, D. R. 2001, *MNRAS*, 327, 1111.
- Goodman, J. 2003, *MNRAS*, 339, 937.
- Ivanov, P. B., Illarianov, A. F. 1997, *MNRAS*, 285, 394.
- Kato, S. 1990, *PASJ*, 42, 99.
- Katz, J. I. 1997, *ApJ*, 478, 527.
- Kumar, S., Pringle, J. E. 1985, *MNRAS*, 213, 435.
- Larwood, J. D. 1997, *MNRAS*, 290, 490.
- Lense, J., Thirring, H. 1918, *Phys. Z.*, 19, 156.
- Liu, S., Melia, F. 2002, *ApJ*, 573, L23.
- Liu, S., Melia, F. 2003, *Astron. Nachr.*, S1, 475.
- Lehto, H. J., Valtonen, M. J. 1996, *ApJ*, 460, 207.
- Melia, F., et al., 2001, *ApJ*, 554, L37.
- Nelson, R. P., Papaloizou, J. C. B. 2000, *MNRAS*, 315, 570.
- Newman, J. A., Eracleous, M., Filippenko, A. V., Halpern, J. P., 1997, *ApJ*, 485, 570.
- Papaloizou, J. C. B., Terquem, C., 1995, *MNRAS*, 274, 987.
- Peterson, B. M., Wanders, I., Bertram, R., et al. 1998, *ApJ*, 501, 82.
- Pringle, J. E. 1996, *MNRAS*, 281, 357.
- Romero, G. E., Chajet, L., Abraham, Z., Fan, J. H. 2000, *A&A*, 360, 57.
- Shakura, N. I., Sunyaev, R. A. 1973, *A&A*, 24, 337.
- Scheuer P. A. G., Feiler R. 1996, *MNRAS*, 282, 291.
- Schödel, R., Ott, T., Genzel, R., et al. 2002, *Nature*, 419, 694.
- Sillanpää, A., Haarala, S., Valtonen, M. J., Sundelius, B., Byrd, G. G. 1988, *ApJ*, 325, 628.
- Stehle, R., Spruit, H. C. 2001, *MNRAS*, 323, 587.

Stirling, A. M., Cawthorne, T. V., Stevens, J. A., et al. 2003, MNRAS, 341, 405.

Storchi-Bergmann, T., Eracleous, M., Livio, M., et al. 1997, ApJ, 489, 87.

Storchi-Bergmann, T., da Silva, R. N., Halpern, J. P., et al. 2003, ApJ, 598, 956.

Thorne, K. S. 1974, ApJ, 191, 507.

Wilkins, D. C. 1972, Phys. Rev. D, 5, 814.

Xie, G. Z., Liang, E. W., Xie, Z. H., Dai, B. Z. 2002, ApJ, 123, 2352.

Zhao, J. -H., Bower, G. C., Goss, W. M. 2001, ApJ, 547, L29.

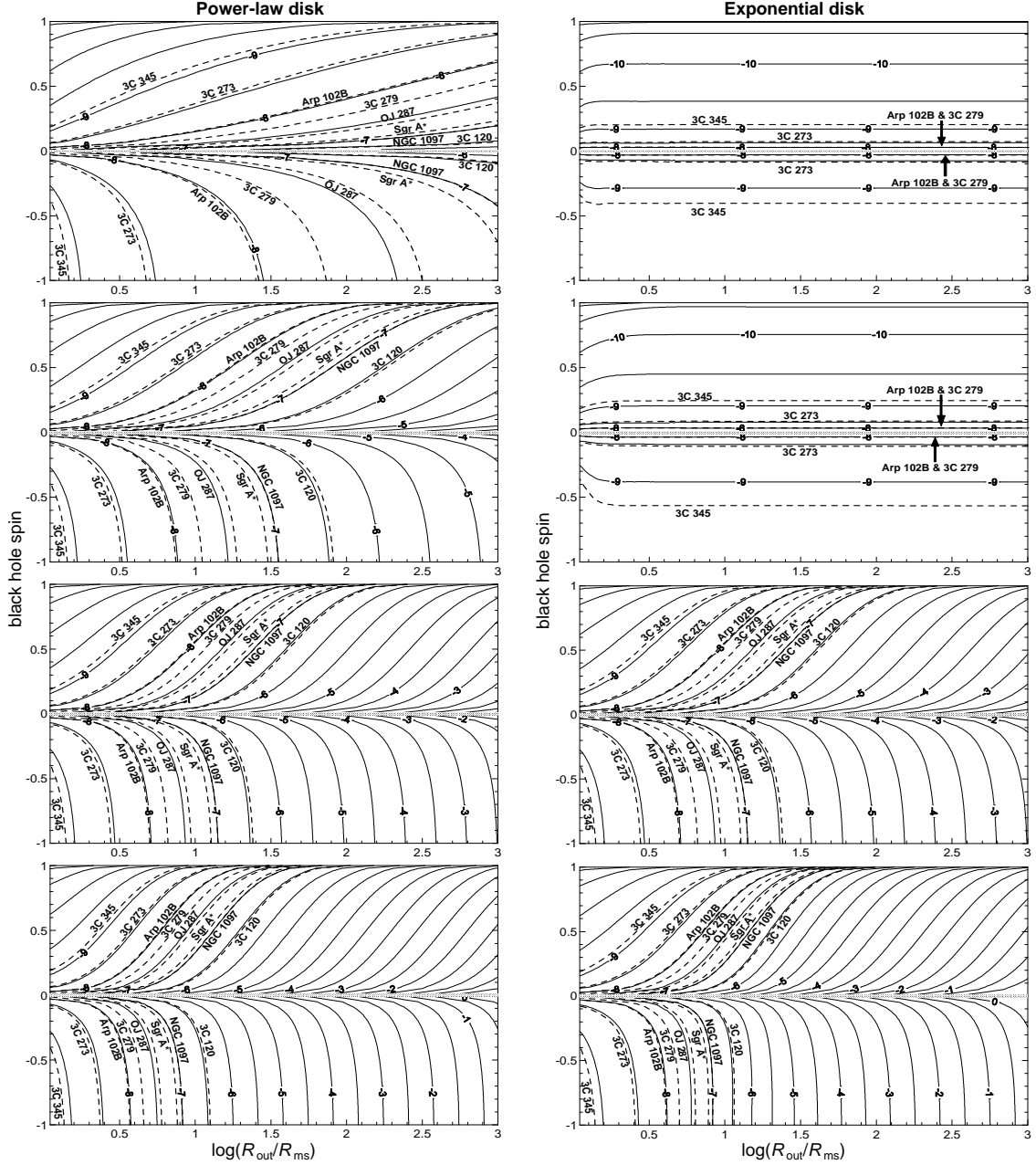


Fig. 1.— Iso-contours (in logarithm scale) of the ratio between the disk precession period and the black hole mass (in units of $\text{yr } M_{\odot}^{-1}$) in the plane defined by the black hole spin and the disk outer radius, for a spin-induced precession model. Left panel corresponds to a power law surface density profile ($s=-2, -1, 0$ and 2 , from top to bottom) and right panel to an exponential disk ($\sigma=-2, -1, 0$ and 0.05 , from top to bottom). The contours of the eight sources studied in this work are represented by dashed lines. The parameter range $-0.01 \leq a_* \leq 0.01$, for which the solutions for the outer radius become very small, were excluded from our calculations.

Table 1. Physical parameters of the sources.

Object	z	$P_{\text{prec}}^{\text{obs}}$ (yr) ^a	Ref.	M_{BH} (M_{\odot})	Ref.	$P_{\text{prec}}/M_{\text{BH}}$ ($\text{yr } M_{\odot}^{-1}$)
Sgr A*	0.000	0.29	(1)	3.70×10^6	(9)	7.84×10^{-8}
NGC 1097	0.004	5.5	(2)	5.50×10^7	(2)	9.96×10^{-8}
Arp 102B	0.024	2.2	(3)	2.20×10^8	(3)	9.59×10^{-9}
3C 120	0.033	12.3	(4)	3.40×10^7	(10)	3.50×10^{-7}
3C 273	0.158	16.0	(5)	4.93×10^9	(11)	2.80×10^{-9}
OJ 287	0.306	11.6	(6)	2.29×10^8	(12)	3.88×10^{-8}
3C 279	0.536	22.0	(7)	8.17×10^8	(11)	1.75×10^{-8}
3C 345	0.593	10.1	(8)	7.96×10^9	(11)	7.97×10^{-10}

Note. — z is the redshift and $P_{\text{prec}}^{\text{obs}}$ is the precession period measured in the observer’s reference frame [$P_{\text{prec}}^{\text{obs}} = (1 + z)P_{\text{prec}}$].

References. — (1) Zhao, Bower & Goss 2001; (2) Storchi-Bergmann et al. 2003; (3) Newman et al. 1997; (4) Caproni & Abraham 2004b; (5) Abraham & Romero 1999; (6) Abraham 2000; (7) Abraham & Carrara 1998; (8) Caproni & Abraham 2004a; (9) Schödel et al. 2002; (10) Peterson et al. 1998; (11) Gu, Cao & Jiang 2001; (12) Xie et al. (2002).